Cong Qi[1]
e-mail: qicongkevin@163.com

Yurong He[1]
e-mail: rong@hit.edu.cn

Yanwei Hu
e-mail: hywhit@foxmail.com

Juancheng Yang
e-mail: yangjc@hit.edu.cn

Fengchen Li
e-mail: lifch@hit.edu.cn

School of Energy Science and Engineering,
Harbin Institute of Technology,
Harbin 150001, China

Yulong Ding
Institute of Particle Science and Engineering,
University of Leeds,
Leeds LS2 9JT, United Kingdom
e-mail: y.ding@leeds.ac.uk

Natural Convection of Cu-Gallium Nanofluid in Enclosures

In this work, the natural convection heat transfer of Cu-gallium nanofluid in a differentially heated enclosure is investigated. A single-phase model is employed with constant or temperature-dependent properties of the fluid. The results are shown over a wide range of Grashof numbers, volume fractions of nanoparticles, and aspect ratios. The Nusselt number is demonstrated to be sensitive to the aspect ratio. It is found that the Nusselt number is more sensitive to thermal conductivity than viscosity at a low velocity (especially for a low aspect ratio and a low Grashof number), however, it is more sensitive to the viscosity than the thermal conductivity at a high velocity (high aspect ratio and high Grashof number). In addition, the evolution of velocity vectors, isotherms, and Nusselt number for a small aspect ratio is investigated. [DOI: 10.1115/1.4004431]

Keywords: Cu-gallium nanofluid, convection heat transfer, enclosure, Grashof number, volume fractions, aspect ratios

1 Introduction

Natural convection heat transfer has been widely studied due to its applications in the cooling of electronics, heat exchangers, solidification and melting, crystal growth, and so on. Holtzman et al. [1] investigated the natural convection of air in an isosceles triangular enclosure.

In order to improve the effect of heat transfer, an innovative technique using nanoscale particles dispersed in a base fluid, known as nanofluid, has been studied extensively during recent years [2–7]. Kim et al. [8] investigated the effect of the suspended particle size on the heat transfer property of nanofluids using the transient hot-wire method. Jang and Choi [9] investigated the effect of nanoparticle size, volume fraction, and temperature on nanofluid thermal conductivity by a dynamic model containing new concepts and simplifying assumptions. Wang and Wei [10] produced several kinds of nanofluid using a chemical solution method and proposed a theory of macroscale heat conduction in nanofluids. Kim et al. [11] presented a study on water-based nanofluids containing alumina, zinc-oxide, and diamond nanoparticles in flow boiling. Nnanna [12] investigated the heat transfer characteristics of buoyancy-driven Al_2O_3-water nanofluids. Milanova and Kumar [13] showed an investigation on the silica nanofluids in pool boiling and also studied the effect of acidity on the heat transfer characteristics of nanofluids. Kim et al. [14] performed an experiment to attempt to reveal that there is an enhancement by adding a few alumina nanoparticles to water in flow boiling. Shukla and Dhir [15] developed a simple model for predicting thermal conductivity of nanofluid and investigated the effect of Brownian motion on thermal conductivity of nanofluid. Lai et al. [16] presented the convection heat transfer performance of γ-Al_2O_3-water in a single 1.02-mm inner diameter with constant heat flux stainless steel tube. Ding et al. [17] investigated the heat transfer behavior of aqueous suspensions of multiwalled carbon nanotubes (CNT nanofluids) flowing through a horizontal tube.

Li and Peterson [18] experimentally investigated the heat transfer behavior of Al_2O_3/water nanofluid with different volume fractions. Aminossadati and Ghasemi [19] numerically studied the natural convection of nanofluid in an enclosure with a heat source on the bottom wall by a finite volume approach using the SIMPLE algorithm. Chang et al. [20] experimentally investigated the natural convection of Al_2O_3 microparticle aqueous suspensions in thin enclosures at three different inclination angles. Nield and Kuznetsov [21] studied the onset of natural convection in a horizontal nanofluid layer using the linear instability theory and a model incorporating the effects of Brownian motion and thermophoresis. Abu-Nada and Chamkha [22] presented a study on natural convection of CuO-EG-water nanofluid in a differentially heated enclosure for a wide range of Rayleigh numbers, volume fractions of nanoparticles, and aspect ratios. Hwang et al. [23] investigated the natural convection thermal characteristics of Al_2O_3-water nanofluid in a rectangular cavity heated from below and compared the theoretical results with experimental results. Ho et al. [24] showed the influences of uncertainties on the heat transfer characteristics of Al_2O_3-water nanofluid due to using different formulas for the effective thermal conductivity and dynamic viscosity. Based on SIMPLE algorithm method, Esfahani and Bordbar [25] studied the double diffusive natural convection in a square filled with nanofluids containing various nanoparticles. Kargar et al. [26] used computational fluid dynamics and artificial neural network to investigate the cooling performance of electronic components in an enclosure filled with nanofluid. Wu and Wang [27] applied semi-implicit projection finite element method and Brinkman–Forcheimer-extended Darcy model to investigate the laminar mixed convection heat transfer across a heated square porous cylinder in different channels.

All the works mentioned above are applications and research on traditional nanofluids made by dispersing nanoparticles in an ordinary liquid such as water, ethylene glycol, or oil with the expectation to obtain higher thermal conductivities [28]. Liquid metal nanofluids are different from the traditional nanofluids. Compared with the traditional nanofluids, liquid metal nanofluids have a much higher thermal conductivity, a smaller density difference between the nanoparticles and the base fluid. As is known, gallium is a typical material, which would stay in a liquid state at near room temperature. In particular, liquid gallium has merits including being

[1] Corresponding author.

Contributed by the Heat Transfer Division of ASME for publication in the JOURNAL OF HEAT TRANSFER. Manuscript received November 2, 2010; final manuscript received June 10, 2011; published online October 6, 2011. Assoc. Editor: Robert D. Tzou.

noncaustic to most materials, nonpoisonous, having a high thermal conductivity and a relatively low viscosity. However, investigations of natural convection heat transfer using liquid metal nanofluids are still scarce and the subject has received very little attention. In view of this, natural convection of Cu-gallium nanofluids in enclosures is investigated in this work. The enhancement in heat transfer, velocity vectors and isotherms for Cu-gallium nanofluids in enclosures are evaluated under a wide range of temperatures, a wide range of volume fractions of nanoparticles and different aspect ratios (W/H) of enclosures.

2 Theoretical Model

The natural convection heat transfer of a Cu-gallium nanofluid in different enclosures is simulated using a single-phase model and the Boussinesq hypothesis with appropriate control equations and boundary conditions.

Considering that liquid metal nanofluids can be assumed as being a continuous medium, the control equations are as follows:

Continuity equation

$$\frac{\partial \rho}{\partial t} + \nabla \cdot (\rho \boldsymbol{u}) = 0 \tag{1}$$

where $\boldsymbol{u}$ is the velocity vector of the Cu-gallium nanofluid.

Momentum equation

$$\frac{\partial \rho \boldsymbol{u}}{\partial t} + \nabla(\rho \boldsymbol{u}\boldsymbol{u}) = -\nabla p + \mu_l \nabla^2 \boldsymbol{u} - \rho\beta g(T - T_c) \tag{2}$$

where μ_l is the dynamic viscosity of the Cu-gallium nanofluid, β is the thermal expansion coefficient of the Cu-gallium nanofluid, and T_c is the temperature of the wall.

Energy equation

$$\frac{\partial T}{\partial t} + \mathbf{u} \cdot \nabla T = \frac{\partial}{\partial x}\left(\frac{k}{\rho c_p}\frac{\partial T}{\partial t}\right) + \frac{\partial}{\partial y}\left(\frac{k}{\rho c_p}\frac{\partial T}{\partial t}\right) \tag{3}$$

3 Numerical Method and Simulation Conditions

The enclosure used in the simulation is shown in Fig. 1. The height and the width of the enclosure are given by H and W, respectively. Four edges are made of copper. The left wall is heated and maintained at a constant temperature (T_H) higher than the temperature (T_C) of the right cold wall. The boundary condition of the top wall is set as a free surface with convective heat transfer and heat loss, and the boundary condition of the bottom wall is adiabatic. Three horizontal test lines are selected.

The enclosure is filled with Cu-gallium nanofluid. The thermophysical properties of gallium and Cu are given in Table 1. The nanofluid is assumed as incompressible and no slip wall boundary

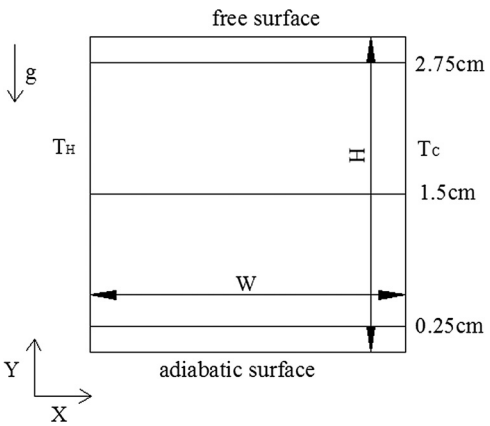

Fig. 1 Schematic of the enclosure

Table 1 Thermophysical properties of Gallium and Cu

Physical properties	Fluid phase (gallium)	Nanoparticles (Cu)
ρ (kg/m^3)	6090	8978
c_p (J/kg k)	429.9–0.275543T	381
μ (m^2/s)	0.0018879	/
K (W m^{-1} K^{-1})	31	387.6

is set. Further, it is idealized that the Cu-gallium nanofluid is a single-phase fluid. The simulation is carried out using quadrilateral uniform grids, SIMPLE algorithm to deal with the coupling of pressure and velocity field, second-order windward difference algorithm to solve momentum equation and energy equation, PRESTO algorithm to process pressure correction equation and appropriate subrelaxation factors [29–31]. The convergence criteria of residual used in the numerical solution is: continuity: 1×10^{-6}, x-velocity: 1×10^{-6}, y-velocity: 1×10^{-6}, energy: 1×10^{-6}.

Xuan and Roetzel [32] proposed a single-phase model that solid particles in nanofluid are ultra fine and are easily fluidized. So the solid particles can be approximately considered as a fluid. Under two assumptions that there exists local thermal equilibrium between the nanoparticles and the base fluid and no motion slip exists between the discontinuous phase of the dispersed ultra fine particles and the continuous liquid, the nanofluid can be seen as a single-phase fluid [32,33]. In this paper, the liquid metal nanofluid is treated as a single-phase fluid, and its physical parameters can be expressed in terms of the properties of the liquid metal and copper nanoparticles, so the equations of the physical parameters of the nanofluid are as follows:

Density equation

$$\rho_{nf} = (1 - \phi)\rho_{bf} + \phi\rho_p \tag{4}$$

where ρ_{nf} is the density of the nanofluid, ϕ is the volume fraction of the Cu nanoparticles, ρ_{bf} is the density of liquid metal, and ρ_p is the density of the Cu nanoparticles. This formula, which is commonly accepted by most researchers, has been found appropriate for use with nanofluids through an experimental validation by Pak and Cho [34].

For heat capacity equation, Pak and Cho [34] have suggested

$$c_{pnf} = (1 - \varphi)c_{pbf} + \varphi c_{pp} \tag{5a}$$

In addition, based on the heat capacity concept, Xuan and Roetzel [32] have proposed

$$(\rho c)_{nf} = (1 - \varphi)(\rho c_p)_{bf} + \varphi(\rho c_p)_p \tag{5b}$$

where c_{pnf} is the heat capacity of nanofluid, c_{pbf} is the heat capacity of liquid metal, and c_{pp} is the heat capacity of the Cu nanoparticles.

For dynamic viscosity equation, Brinkman [35] proposed an expression for fluid at low fraction ($\varphi < 0.05$) as follows:

$$\mu_{nf} = \mu_f \times (1 + 2.5 \times \varphi) \tag{6a}$$

The above dynamic viscosity equation was extended by Brinkman [35] for high volume fraction ($\varphi > 0.05$) as follows:

$$\mu_{nf} = \frac{\mu_f}{(1 - \phi)^{2.5}} \tag{6b}$$

Other relations have been proposed in the literature with their own limitations and applications [36]. A polynomial curve fitting on the experimental data was carried out by Wang et al. [37] as follows:

$$\mu_{nf} = \mu_f \times \left(123 \times \varphi^2 + 7.3 \times \varphi + 1\right) \tag{6c}$$

where μ_{nf} is the viscosity of nanofluid and μ_f is the viscosity of the liquid metal.

Hamilton and Crosser [38] proposed a thermal conductivity equation

$$k_{nf} = k_f \left[\frac{(k_p + 2k_f) - 2\phi(k_f - k_p)}{(k_p + 2k_f) + \phi(k_f - k_p)} \right] \quad (7a)$$

Yu and Choi [39] proposed another thermal conductivity equation

$$k_{nf} = k_f \left[\frac{(k_p + 2k_f) + 2(k_p - k_f)(1+\beta)^3\phi}{(k_p + 2k_f) - 2(k_p - k_f)(1+\beta)^3\phi} \right] \quad (7b)$$

where k_{nf} is the thermal conductivity of the nanofluid, k_f is the thermal conductivity of the liquid metal, and β is the ratio of the nanolayer thickness to the original particle radius.

It is shown that Brinkman model underestimates the effective viscosity of the nanofluid compared with other expressions [40]. The fact that none was specifically developed for nanofluids can cause the substantial differences between the predictions of these different expressions for thermophysical properties. In addition, there are considerable uncertainties with respect to their concentration in reality, but they are all based on the assumption that nanoparticles are uniformly distributed throughout the base fluid. Finally, these expressions do not account for the effects of the size disparity between the nanoparticles, and the size is an important factor for heat transfer [41].

In this paper, Eq. (4) is used for the density, Eq. (5*a*) is used for the specific heat, Eq. (6*b*) is used for the viscosity, and Eq. (7*a*) is used for the conductivity. This is the same combination used by Gosselin and Silva [42] in their optimization study and is identified as the GdS combination hereafter.

The Nusselt number can be expressed as

$$Nu = \frac{hH}{k_{nf}} \quad (8)$$

The heat transfer coefficient is computed from

$$h = \frac{q_w}{T_H - T_L} \quad (9)$$

The thermal conductivity of the nanofluid is defined by

$$k_{nf} = -\frac{q_w}{\partial T/\partial x} \quad (10)$$

Substituting Eqs. (9) and (10) into Eq. (8), the local Nusselt number along the left wall can be written as

$$Nu = -\left(\frac{\partial T}{\partial x}\right) \cdot \frac{H}{T_H - T_L} \quad (11)$$

The average Nusselt number is determined from

$$Nu_{avg} = \int_0^1 Nu(y)dy \quad (12)$$

The Grashof number is based on nanofluid properties and is defined by

$$Gr = \frac{g\alpha\Delta t l^3}{\nu^2} \quad (13)$$

The Prandtl number is defined by

$$Pr = \frac{\nu}{a} = \frac{c_{p_{nf}}\mu_{nf}}{k_{nf}} \quad (14)$$

Table 2 Comparison of the mean Nusselt number along the left wall with different grids

Physical properties	60×60	80×80	100×100	120×120
Nu_{avg}	21.3292	21.2856	20.9913	21.0056

For variable properties in FLUENT®6.3 software, because FLUENT software can directly use user-defined function, so user-defined functions of variable properties are programmed and introduced to solve the variable properties.

Because the thermal expansion coefficient of solid-Cu ($1.22 \times 10^{-5} - 1.89 \times 10^{-5}$) is much lower than that of liquid-Ga (1.0×10^{-4}), in addition, the volume fraction of Cu is small, also we have tested the results with considering the thermal expansion coefficient of solid-Cu, and it is found that the results are almost the same with those without considering the thermal expansion coefficient of solid-Cu, so the liquid metal Ga is approximately treated as the thermal expansion coefficient of nanofluid in this paper.

4 Results and Discussion

As shown in Table 2, the grid independence test is performed using successively sized grids, 60×60, 80×80, 100×100, and 120×120 at $Gr = 3 \times 10^6$, $\varphi = 0.00$ (pure liquid metal gallium). From Table 2, it can be seen that there is a distinct difference from the numerical results with grids 60×60 and 80×80 to that with grids 100×100 and 120×120, but there is little change in the results between the grids 100×100 and 120×120. In order to accelerate the simulation, a grid size of 100×100 is chosen as the suitable one, which can guarantee a grid independent solution.

Initial simulations were carried out on pure liquid metal gallium to check the reliability and accuracy of the numerical methods and parameter settings in the FLUENT 6.3® environment. The temperature data and velocity data on horizontal direction test lines $Y = 2.75$ cm, $Y = 1.5$ cm, and $Y = 0.25$ cm are, respectively, compared with numerical and experimental data [29]. The results are shown in Figs. 2 and 3. It can be seen from Fig. 2 that reasonably good agreement has been achieved on horizontal direction test lines $Y = 1.5$ cm and $Y = 0.25$ cm, but there is certain deviation between numerical simulation results and experimental results on horizontal direction test line $Y = 2.75$ cm. Because the top wall is a free surface, and it is difficult to determine its heat transfer coefficient, it is not easy to obtain a temperature distribution line, which is in good agreement with experimental results. However, the general trend is the same, and the simulation results in this paper have a good agreement with the simulation results in literature [29]. In view of this, the temperature distribution on horizontal

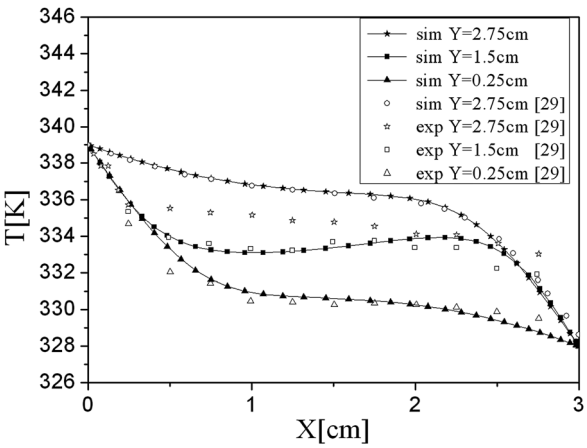

Fig. 2 Comparison between present work and other published data for the temperature distribution at different *Y*

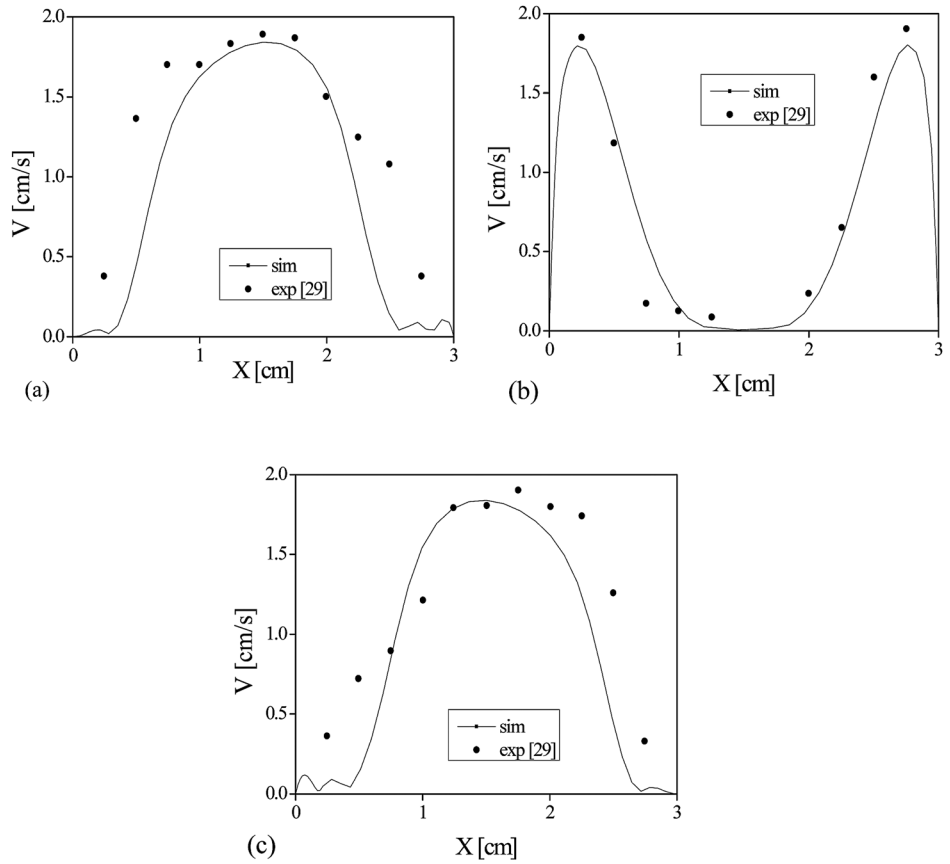

Fig. 3 Comparison between present work and other published data for the velocity distribution at different Y (*a*) $Y = 2.75$ cm; (*b*) $Y = 1.5$ cm; (*c*) $Y = 0.25$ cm

direction test line $Y = 2.75$ cm is accepted. It can be seen from Fig. 3 that reasonably good agreement has been achieved on horizontal direction test lines $Y = 2.75$ cm, $Y = 1.5$ cm, and $Y = 0.25$ cm. Having built up the confidence in the model and parameter setting in the FLUENT 6.3® environment, systematic simulations are performed on Cu-gallium nanofluids.

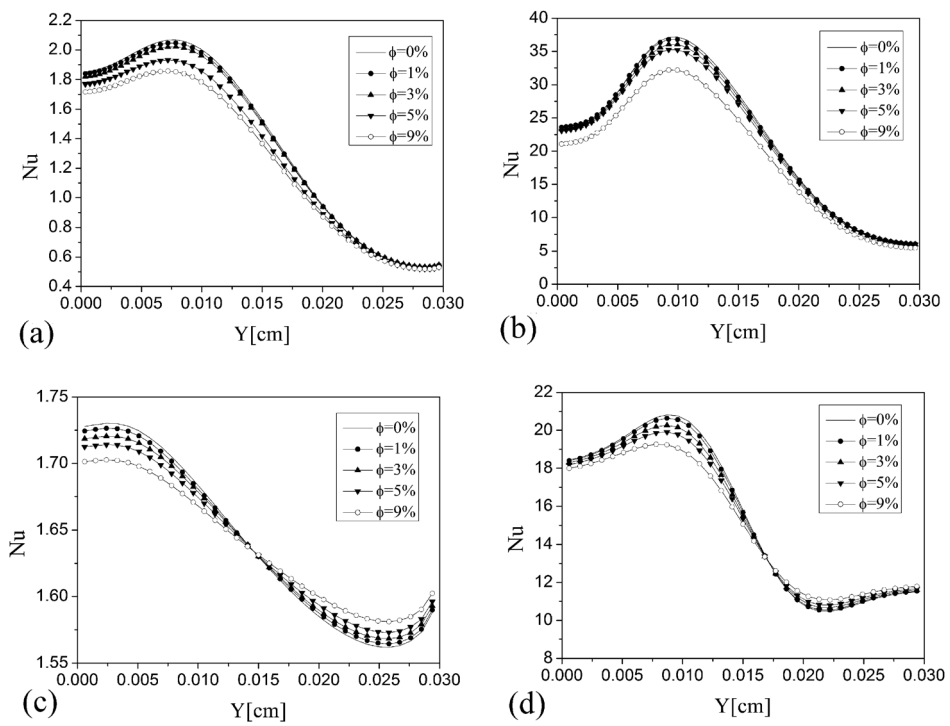

Fig. 4 Nusselt number distribution along the heated surface using Cu-Ga nanofluid (*a*) $Gr = 3 \times 10^5$, $A = 1$; (*b*) $Gr = 3 \times 10^6$, $A = 1$; (*c*) $Gr = 3.75 \times 10^4$, $A = 0.5$; (*d*) $Gr = 3.75 \times 10^5$, $A = 0.5$

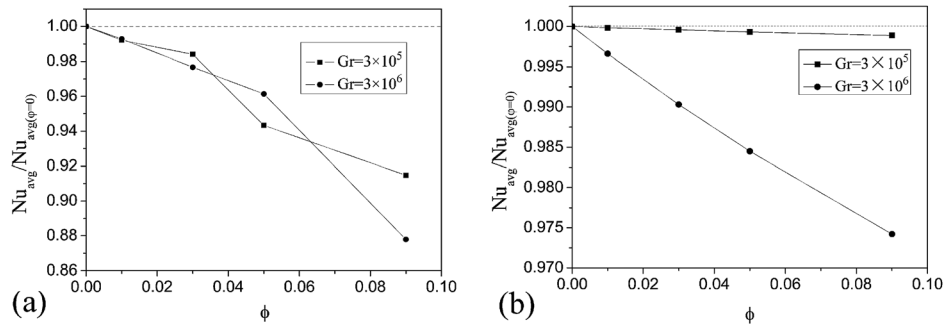

Fig. 5 Average Nusselt number ratio between nanofluid and pure liquid metal Ga at different Grashof numbers (*a*) $A = 1$; (*b*) $A = 0.5$

Figure 4 illustrates the Nusselt number distribution along the heated surface for different Grashof numbers and different aspect ratios of the enclosure. As outlined in Figs. 4(*a*) and 4(*b*), it is clear that the Nusselt number distribution along the heated surface decreases with the volume fraction of nanoparticles for $A = 1$. For the case of $\mathrm{Gr} = 3 \times 10^5$ and $\mathrm{Gr} = 3 \times 10^6$, high values of φ cause the fluid to become more viscous, which causes the velocity to decrease accordingly resulting in a reduced convection for $A = 1$. As shown in Figs. 4(*c*) and 4(*d*), it is observed that the addition of nanoparticles causes the Nusselt number distribution along the heated surface to decrease for $y < 0.015$ cm and to increase for $y > 0.015$ cm with $A = 0.5$.

Figure 5 presents the average Nusselt number ratio between nanofluid and pure liquid metal Ga at different Grashof numbers and aspect ratios. It is observed that the average Nusselt number decreases with the volume fraction of nanoparticles for $A = 1$ and $A = 0.5$. In addition, it can be seen that the average Nusselt number decreases less at a low Grashof number and low aspect ratio than that at a high Grashof number and a high aspect ratio.

Figure 6 illustrates the evolution of velocity vectors and isotherms with time using Cu-Ga nanofluid at $\mathrm{Gr} = 4.7 \times 10^3$ for $A = 0.25$ and $\varphi = 0.03$. It is observed that the vortex has not been formed, and the isotherms are parallel to the heated surface at the start stage (Figs. 6(*a*)–6(*c*)), then one big vortex gradually forms (Fig. 6(*d*)), with passing time, one big vortex gradually changes into three big vortices(Figs. 6(*e*) and 6(*f*)), and then the three big vortexes evolve into two big vortices again with some small vortices(Figs. 6(*g*) and 6(*h*)). In addition, the isotherms become crooked with time.

Shown in Fig. 7 is the evolution of Nusselt number distribution along the heated surface with time using Cu-Ga nanofluid at $\mathrm{Gr} = 4.7 \times 10^3$ for $A = 0.25$. It is interesting to note that there is

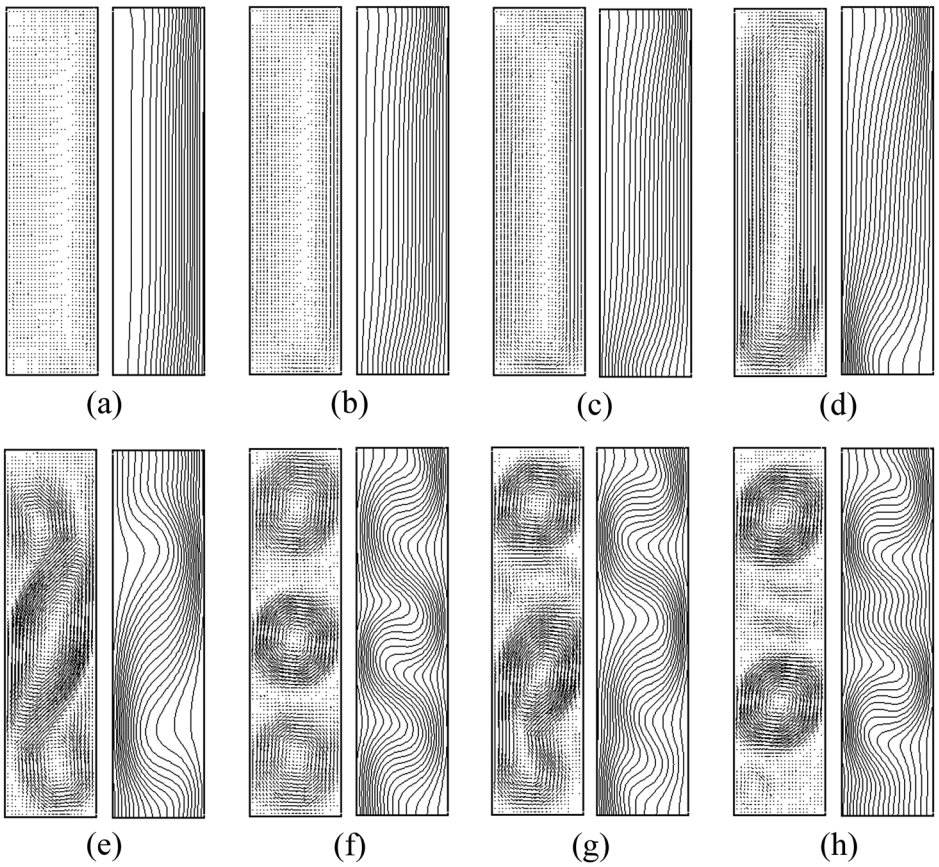

Fig. 6 The evolution with time of velocity vectors (on the left, →0.6 cm/s) and isotherms (on the right) using Cu-Ga nanofluid at $\mathrm{Gr} = 4.7 \times 10^3$, $A = 0.25$ and $\phi = 0.03$ (*a*) $t = 30$ s; (*b*) $t = 50$ s; (*c*) $t = 70$ s; (*d*) $t = 150$ s; (*e*) $t = 300$ s; (*f*) $t = 550$ s; (*g*) $t = 700$ s; (*h*) $t = 1040$ s

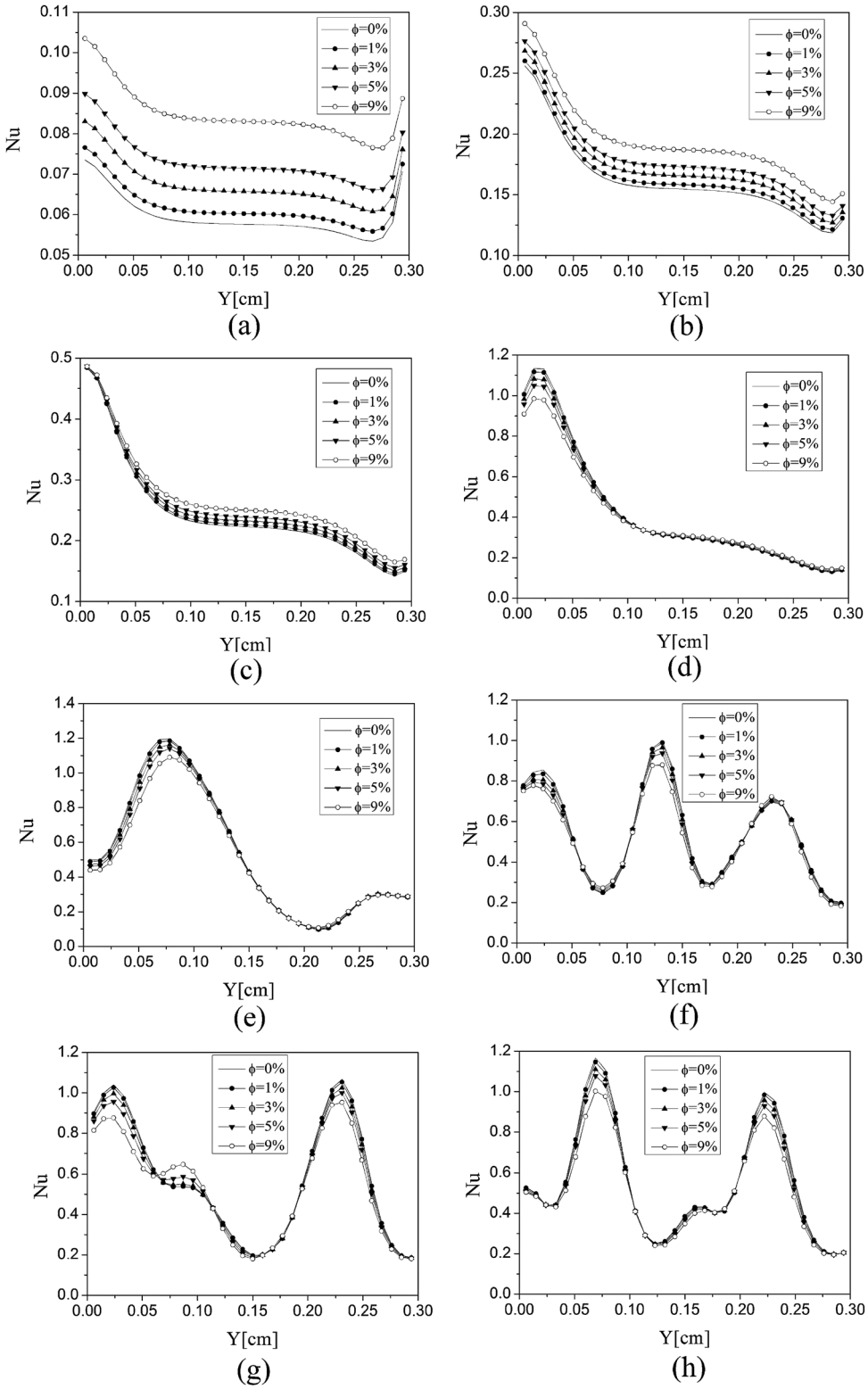

Fig. 7 The evolution with time of Nusselt number distribution along the heated surface using Cu-Ga nanofluid at Gr = 4.7×10^3, $A = 0.25$ (*a*) $t = 30$ s; (*b*) $t = 50$ s; (*c*) $t = 70$ s; (*d*) $t = 150$ s; (*e*) $t = 300$ s; (*f*) $t = 550$ s; (*g*) $t = 700$ s; (*h*) $t = 1040$ s

an enhancement in the Nusselt number distribution along the heated surface when using a higher volume fraction of nanoparticles at the early stage (before 70 s); there are a deterioration in the Nusselt number for one segment of y and an enhancement in the Nusselt number for the other segment of y between 70 s and 300 s, which is similar to the distribution in Figs. 4(*c*) and 4(*d*); and there is a reduction in the Nusselt number at a later time (after 300 s). It takes a longer time to form into one big vortex for $A = 0.25$ than for $A = 1$ or $A = 0.5$, accordingly, the velocity at the early stage (before 70 s) for $A = 0.25$ is lower than that for $A = 1$ or $A = 0.5$. The heat transfer is dominated by conduction at a low velocity and by convection at a high velocity. The effect of the

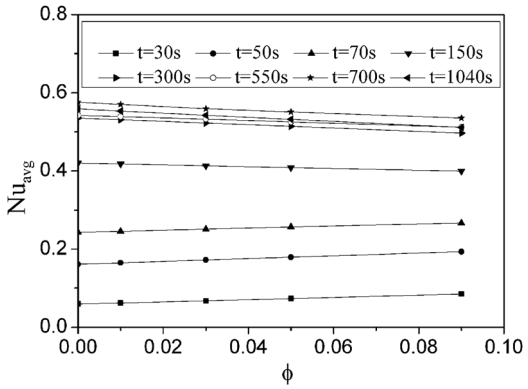

Fig. 8 Average Nusselt number at different time for $Gr = 4.7 \times 10^3$ and $A = 0.25$

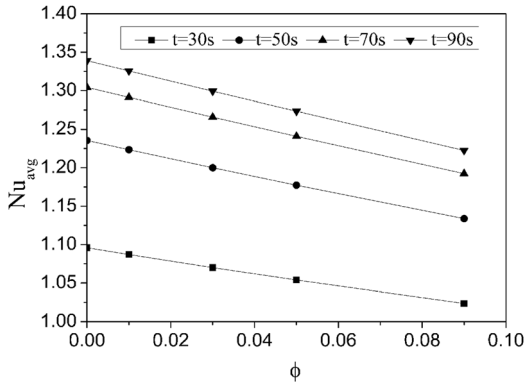

Fig. 10 Average Nusselt number at different time for $Gr = 3 \times 10^5$ and $A = 1$

viscosity becomes clearer at higher velocity, which will reduce the convection currents and accordingly diminish the temperature gradient and the Nusselt number distribution along the heated surface. This explains why there is an enhancement by adding nanoparticles at an early stage for $A = 0.25$ (Figs. 10(*a*)–10(*c*)) and there is no enhancement for $A = 1$ or $A = 0.5$ (Fig. 4). The velocity becomes high, and the heat transfer is dominated by convection between 70 s and 300 s for $A = 0.25$, so there appears the phenomenon that there is an enhancement for one section of y and a reduction for another section of y for $A = 0.25$, which is similar to what happens for $A = 0.5$. The velocity becomes much higher after 300 s, and there is a reduction by adding nanoparticles, which is similar to what happens for $A = 1$.

Figure 8 contains the average Nusselt number at different time for $Gr = 4.7 \times 10^3$ and $A = 0.25$. It is obvious to see that the average Nusselt number increases with the volume fraction of nanoparticles before 70 s. After 70 s, the nanofluid is more sensitive to viscosity, so the average Nusselt number decreases with the volume fraction of nanoparticles. However, it is observed that the average Nusselt number at 1040 s is smaller than it is at 700 s, this can be explained in Figs. 6(*g*) and 6(*h*). There are three big vortices in Fig. 6(*g*), as time passes, only two big vortices remain in Fig. 6(*h*). The distance between vortexes in Fig. 6(*h*) is longer than it in Fig. 6(*g*), and the areas between the vortices in Fig. 6(*h*) are larger than those in Fig. 6(*g*), further more, the velocity in these areas is lower than it in the vortices, so the low velocity reduces the convection and accordingly diminishes the average Nusselt number.

Figure 9 presents the average Nusselt number at different time for $Gr = 3.75 \times 10^4$ and $A = 0.5$. Figure 10 illustrates the average Nusselt number at different time for $Gr = 3 \times 10^5$ and $A = 1$. It is observed that the average Nusselt number decreases with the volume fraction of nanoparticles at different time for both $A = 0.5$ and $A = 1$, in addition, the average Nusselt number for $A = 0.5$ decreases less than that for $A = 1$.

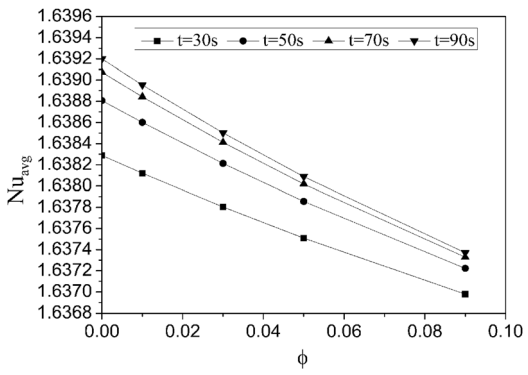

Fig. 9 Average Nusselt number at different time for $Gr = 3.75 \times 10^4$ and $A = 0.5$

5 Conclusions

The natural convection heat transfer of Cu-gallium nanofluid in an enclosure is investigated. A single-phase model is employed with constant or temperature-dependent properties of the fluid. The following results are obtained in this work:

For an enclosure with a width to height ratio $A = 1$, the Nusselt number of Cu-Ga nanofluid along the heated surface is reduced when increasing the volume fraction of nanoparticles. With decreasing aspect ratio, for $A = 0.5$, the Nusselt number of Cu-Ga nanofluid is reduced when increasing the volume fraction of nanoparticles for $y < 0.015$ (half of the heated surface), in contrast, the Nusselt number is enhanced when increasing the volume fraction of nanoparticles for $y > 0.015$. For a low aspect ratio ($A = 0.25$), the Nusselt number is reduced at a later stage (after 300 s) but is enhanced at an early stage (before 70 s). The Nusselt number is demonstrated to be sensitive to the aspect ratio. It is observed that the Nusselt number is more sensitive to thermal conductivity than viscosity at a low velocity (especially at an early stage for a low aspect ratio and a low Grashof number), however, it is more sensitive to viscosity than the thermal conductivity at a high velocity (high aspect ratio and high Grashof number). In addition, the evolution of velocity vectors and isotherms for a small aspect ratio ($A = 0.25$) is obtained, it is found that the velocity field evolves from one big vortex to three big vortices, and finally forms two big vortices.

Acknowledgment

This work is financially supported by Program for New Century Excellent Talents in University NCET-08-0159, Natural Science Foundation of China through Grant No. 51076036, the Scientific and Technological foundation for distinguished returned overseas Chinese scholars and the Key Laboratory Opening Funding (HIT.KLOF.2009039).

Nomenclature

A = aspect ratio (W/H)
c_p = heat capacity (J/kg · K)
k = thermal conductivity (W m^{-1} K^{-1})
h = local heat transfer coefficient (W m^{-2} K^{-1})
Nu = Nusselt number
q_w = heat flux (W m^{-2})
Gr = Grashof number
H = height of the enclosure (m)
W = width of the enclosure (m)
g = gravitational acceleration (m s^{-2})
X, Y = coordinates (m)
t = time (s)

Greek Symbols

ρ = density (kg/m^3)
μ = kinematic viscosity (m^2/s)
φ = nanoparticle volume fraction

Subscripts

C = cold
H = hot
f = fluid
nf = nanofluid
p = particle
w = wall
avg = average

References

[1] Holtzman, G. A., Hill, R. W., and Ball, K. S., 2000, "Laminar Natural Convection in Isosceles Triangular Enclosures Heated From Below and Symmetrically Cooled From Above," ASME J. Heat Transfer, **122**, pp. 485–491.
[2] Xuan, Y., and Li, Q., 2003, "Investigation on Convective Heat Transfer and Flow Features of Nanofluids," ASME J. Heat Transfer, **125**, pp. 151–155.
[3] Das, S. K., Putra, N., Thiesen, P., and Roetzel, W., 2003, "Temperature Dependence of Thermal Conductivity Enhancement for Nanofluids," ASME J. Heat Transfer, **125**, pp. 567–574.
[4] Williams, W., Buongiorno, J., and Hu, L. W., 2008, "Experimental Investigation of Turbulent Convective Heat Transfer and Pressure Loss of Alumina/Water and Zirconia/Water Nanoparticle Colloids (Nanofluids) in Horizontal Tubes," ASME J. Heat Transfer, **130**, p. 042412.
[5] Buongiorno, J., 2006, "Convective Transport in Nanofluids," ASME J. Heat Transfer, **128**, pp. 240–250.
[6] Prasher, R., Bhattacharya, P., and Phelan, P. E., 2006, "Brownian-Motion-Based Convective-Conductive Model for the Effective Thermal Conductivity of Nanofluids," ASME J. Heat Transfer, **128**, pp. 588–595.
[7] Vadasz, P., 2006, "Heat Conduction in Nanofluid Suspensions," ASME J. Heat Transfer, **128**, pp. 465–477.
[8] Kim, S. H., Choi, S. R., and Kim, D., 2007, "Thermal Conductivity of Metal-Oxide Nanofluids: Particle Size Dependence and Effect of Laser Irradiation," ASME J. Heat Transfer, **129**, pp. 298–307.
[9] Jang, S. P., and Choi, S. U. S., 2007, "Effects of Various Parameters on Nanofluid Thermal Conductivity," ASME J. Heat Transfer, **129**, pp. 617–623.
[10] Wang, L., and Wei, X., 2009, "Nanofluids: Synthesis, Heat Conduction, and Extension," ASME J. Heat Transfer, **131**, p. 033102.
[11] Kim, S. J., McKrell, T., Buongiorno, J., and Hu, L. W., 2009, "Experimental Study of Flow Critical Heat Flux in Alumina-Water, Zinc-Oxide-Water, and Diamond-Water Nanofluids," ASME J. Heat Transfer, **131**, p. 043204.
[12] Nnanna, A. G. A., 2007, "Experimental Model of Temperature-Driven Nanofluid," ASME J. Heat Transfer, **129**, pp. 697–704.
[13] Milanova, D., and Kumar, R., 2008, "Heat Transfer Behavior of Silica Nanoparticles in Pool Boiling Experiment," ASME J. Heat Transfer, **130**, p. 042401.
[14] Kim, S. J., McKrell, T., Buongiorno, J., and Hu, L. W., 2008, "Alumina Nanoparticles Enhance the Flow Boiling Critical Heat Flux of Water at Low Pressure," ASME J. Heat Transfer, **130**, p. 044501.
[15] Shukla, R. K., and Dhir, V. K., 2008, "Effect of Brownian Motion on Thermal Conductivity of Nanofluids," ASME J. Heat Transfer, **130**, p. 042406.
[16] Lai, W. Y., Vinod, S., Phelan, P. E., and Prasher, R., 2009, "Convective Heat Transfer for Water-Based Alumina Nanofluids in a Single 1.02-mm Tube," ASME J. Heat Transfer, **131**, 112401.
[17] Ding, Y., Alias, H., Wen, D., and Williams, R. A., 2006, "Heat Transfer of Aqueous Suspensions of Carbon Nanotubes (CNT Nanofluids)," Int. J. Heat Mass Transfer, 49, pp. 240–250.
[18] Li, C. H., and Peterson, G. P., 2010, "Experimental Studies of Natural Convection Heat Transfer of Al_2O_3/DI Water Nanoparticle Suspensions (Nanofluids)," Adv. Mech. Eng., 2010, 742739.
[19] Aminossadati, S. M., and Ghasemi, B., 2009, "Natural Convection Cooling of a Localised Heat Source at the Bottom of a Nanofluid Filled Enclosure," Eur. J. Mech. B/Fluids, **28**, pp. 630–640.
[20] Chang, B. H., Mills, A. F., and Hernandez, E., 2008, "Natural Convection of Microparticle Suspensions in Thin Enclosures," Int. J. Heat Mass Transfer, **51**, pp. 1332–1341.
[21] Nield, D. A., and Kuznetsov, A. V., 2010, "The Onset of Convection in a Horizontal Nanofluid Layer of Finite Depth," Eur. J. Mech. B/Fluids, **29**, pp. 217–223.
[22] Abu-Nada, E., and Chamkha, A. J., 2010, "Effect of Nanofluid Variable Properties on Natural Convection in Enclosures Filled With a CuO-EG-Water Nanofluid," Int. J. Therm. Sci., **49**, pp. 2339–2352.
[23] Hwang, K. S., Lee, J. H., and Jang, S. P., 2007, "Buoyancy-Driven Heat Transfer of Water-Based Al2O3 Nanofluids in a Rectangular Cavity," Int. J. Heat Mass Transfer, **50**, pp. 4003–4010.
[24] Ho, C. J., Chen, M. W., and Li, Z. W., 2008, "Numerical Simulation of Natural Convection of Nanofluidin a Square Enclosure: Effects Due to Uncertainties of Viscosityand Thermal Conductivity," Int. J. Heat Mass Transfer, **51**, pp. 4506–4516.
[25] Esfahani, J. A., and Bordbar, V., 2011, "Double Diffusive Natural Convection Heat Transfer Enhancement in a Square Enclosure Using Nanofluids," ASME J. Nanotechnol. Eng. Med., **2**, p. 021002.
[26] Kargar, A., Ghasemi, B., and Aminossadati, S. M., 2011, "An Artificial Neural Network Approach to Cooling Analysis of Electronic Components in Enclosures Filled With Nanofluids," ASME J. Electron. Packag., **133**, p. 011010.
[27] Wu, H. W., and Wang, R. H., 2011, "Mixed Convective Heat Transfer Past a Heated Square Porous Cylinder in a Horizontal Channel With Varying Channel Height," ASME J. Heat Transfer, **133**, p. 022503.
[28] Ma, K. Q., and Liu, J., 2007, "Nano Liquid-Metal Fluid as Ultimate Coolant," Phys. Lett. A, **361**, pp. 252–256.
[29] Xu, B., and Li, B. Q., 2005, "Hot-Film Measurement of Temperature Gradient Induced Natural Convection in Liquid Gallium," Exp. Therm. Fluid Sci., **29**, pp. 697–704.
[30] Pan, B., Shang, D. Y., Li, B. Q., and Groh, H. C. D., 2002, "Magnetic Filed Effects on G-Jitter Induced Flow and Solute Transport," Int. J. Heat Mass Transfer, **45**, pp. 125–144.
[31] Alexander, J. I. D., Amiroudine, S., Ouazzani, J., and Rosenberger, F., 1991, "Analysis of the Low Gravity Tolerance of Bridgman-Stockbarger Crystal Growth II: Transient and Periodic Accelerations," J. Cryst. Growth, **113**, pp. 21–38.
[32] Xuan, Y., and Roetzel, W., 2000, "Conceptions for Heat Transfer Correlation of Nanofluids," Int. J. Heat Mass Transfer, **43**, pp. 3701–3707.
[33] Maliga, S. E. B., Palm, S. M., Nguyen, C. T., Roy, G., and Galanis, N., 2005, "Heat Transfer Enhancement Using Nanofluid in Forced Convection Flow," Int. J. Heat Fluid Flow, **26**, pp. 530–546.
[34] Pak, B. C., and Cho, Y. I., 1998, "Hydrodynamic and Heat Transfer Study of Dispersed Fluids With Submicron Metallic Oxide Particles," Exp. Heat Transfer, **11**, pp. 151–170.
[35] Brinkman, H. C., 1952, "The Viscosity of Concentrated Suspensions and Solutions," J. Chem. Phys., **20**, pp. 571–581.
[36] Drew, D. A., and Passman, S. L., 1999, *Theory of Multicomponent Fluids*, Springer, Berlin.
[37] Wang, X., Xu, X., and Choi, S. U. S., 1999, "Thermal Conductivity of Nanoparticles-Fluid Mixture," J. Thermophys. Heat Transfer, **13**, pp. 474–480.
[38] Hamilton, R. L., and Crosser, O. K., 1962, "Thermal Conductivity of Heterogeneous Two-Component Systems," Ind. Eng. Chem. Fundam., **1**, pp. 187–191.
[39] Yu, W., and Choi, S. U. S., 2003, "The Role of Interfacial Layers in the Enhanced Thermal Conductivity of Nanofluids: A Renovated Maxwell Model," J. Nanopart. Res., **5**, pp. 167–171.
[40] Mansour, R. B., Galanis, N., and Nguyen, C. T., 2007, "Effect of Uncertainties in Physical Properties on Forced Convection Heat Transfer With Nanofluids," Appl. Therm. Eng., **27**, pp. 240–249.
[41] Tzou, D. Y., 2008, "Thermal Instability of Nanofluids in Natural Convection," Int. J. Heat Mass Transfer, **51**, pp. 2967–2979.
[42] Gosselin, L., and da Silva, A., 2004, "Combined Heat Transfer and Power Dissipation Optimization of Nanofluid Flow," Appl. Phys. Lett., **85**, pp. 4160–4162.